

# Unbalanced Metamaterials Applied to Phase Shifter: Dedicated Design Method and Application in C-Band

Jonathan Vivos<sup>1, \*</sup>, Thomas Crépin<sup>1</sup>, Michel-François Foulon<sup>2</sup>, and Jérôme Sokoloff<sup>3</sup>

**Abstract**—In order to design differential phase shifters (DPS) from metamaterial-based transmission lines, research had a long tradition of using balanced transmission lines which are a particular case of metamaterials, specifically characterized by a simplified equivalent circuit model. This paper presents an innovative way of designing DPS metamaterials by exploiting metamaterial properties more widely, using both balanced and unbalanced cases to obtain a broader set of solutions. These solutions are acquired through the dedicated method this paper expounds, and conceived with the help of a new use of metamaterials. For the sake of ensuring time efficiency and implementation easiness of this design method for industrial purpose, the full wave parametric optimization is reduced to its minimum by exploiting as much as possible in analytic parametric study. This method is illustrated by an application of 180° DPS on C-Band (5–6 GHz). Three prototypes were fabricated, and the measurements show that the best case of DPS has less than 9° of phase error over the targeted 20% bandwidth, with a return loss less than –14 dB and insertion losses lower than 1 dB.

## 1. INTRODUCTION

As of today, Differential Phase Shifters (DPS) are required in a lot of communication systems such as phased array antennas or power combiners. DPS could be described as follows: a four ports network composed of two lines, respectively called the reference line and main line.

The aim of the DPS is to have a constant phase shift between these lines over a specified bandwidth. The most typical DPS consists in two Transmission Lines (TL) of different length. These systems suffer from large size and their bandwidth is limited due to their different phase slope. Broadband passive DPS can be obtained by Schiffman phase shifters [1], i.e., by folding the main line, thus creating a coupling section. However, these DPS still require large circuit area at least in L and C-bands and the topology of their design depends on their phase shift and is generally used for particular cases such as 90° DPS.

Arbitrary phase shifts can be obtained by using tunable elements such as varactors [2] to control the phase shift by changing the voltage. These systems are called analog DPS. Arbitrary phase shifts can also be obtained with digital DPS, which are composed of phase shifters (22.5°, 45°, 90°) linked by switches [3]. Both of these structures can achieve arbitrary phase shifts on quite large bandwidth but their fabrication is complex and expensive.

Over the last years, the use of metamaterials has earned significant interest in the design of small-size and low-cost microwave devices, with unique properties. Metamaterials (also called left handed materials) were first introduced by Veselago [4] in 1968, and were known as materials exhibiting simultaneously negative permittivity and permeability. Since then, their use as transmission lines loaded

---

*Received 13 February 2019, Accepted 27 April 2019, Scheduled 30 May 2019*

\* Corresponding author: Jonathan Vivos (jonathan.vivos@onera.fr).

<sup>1</sup> ONERA/DEMR, Université de Toulouse, Toulouse, France. <sup>2</sup> Thales Alenia Space, Toulouse, France. <sup>3</sup> LAPLACE, Université de Toulouse, CNRS, INPT, UPS, France.

by lumped capacitance and inductance was more thoroughly studied by Caloz and Itoh [5] as Composite Right Left Handed Transmission Lines (CRLH-TL) and by Eleftheriades and Balmain [6].

These reference papers have provided a better theoretical grasp of these lines, thus enabling design methods of CRLH-TL to be introduced, particularly [7] when aiming at design a CRLH-TL directly from its equivalent circuit model. The use of CRLH balanced lines has led to the design of metamaterial phase shifters. CRLH balanced lines are particular cases of CRLH-TLs with no central forbidden bandgap, which provides a simplified equivalent circuit model and a direct link between electrical elements and phase values. These CRLH balanced lines have been particularly applied for several purposes, such as: achieving dual band phase shift [8] for dual band couplers, targeting an arbitrary phase shift [9] and achieving both phase and phase slope control [10].

Metamaterial lines have also been a key element for the design of digital DPS for arbitrary phase shift ( $0-90^\circ$ ). To do so, they use another approach based on the use of Complementary Split Ring Resonators [CSRR] loaded microstrip lines [11, 12].

This paper presents an original way of exploiting metamaterials more widely by creating multiple solutions using central forbidden bandgap as degree of freedom, without changing the phase velocity at working frequencies. Through this use of unbalanced lines, multiple geometries are obtained, either with improved compactness or with return loss compared to the equivalent balanced case commonly used. This concept, combined with previous studies of CRLH-TLs, leads to a design method extracting several possible metamaterial DPS from an arbitrary phase shift required over a specified bandwidth. Different performances are obtained in term of phase shift value, return loss and compactness.

This paper is organized with three upcoming sections: Section 2 presents the principle of our dedicated method and the way to derive unbalanced lines for DPS design. Section 3 describes the different steps of this design method. In order to illustrate and validate the method, an application of a  $180^\circ$  DPS with an aim of 20% bandwidth in C-band (5–6 GHz) is considered, several prototypes are designed and characterized. Comparisons between simulated and experimental results are finally shown in Section 4.

## 2. THEORETICAL BACKGROUND AND PRINCIPLE OF THE METHOD

### 2.1. Definition of the Phase Shift Criteria

As briefly described in the introduction, the DPS is defined as a four ports network and more particularly as two separated lines: a reference line and a main line (Figure 1(a)). These two lines have a difference in their designs which affects their phase behavior, hence creating a differential phase shift between them (Figure 1(b), Figure 1(c)). The purpose of the reference line is to establish the standard value of the phase. A basic design is generally selected for this line. In this paper, this line is built as a transmission line.

The design of a DPS consists in shaping and adjusting the main line to get the targeted phase

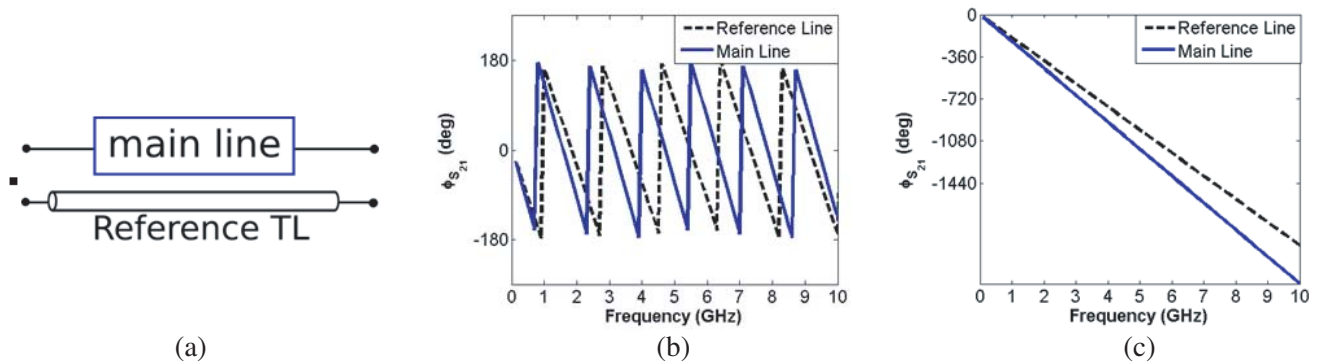


**Figure 1.** (a) Illustration of the concept of DPS, (b) wrapped phase behavior for the reference and main lines of the DPS and (c) unwrapped phase shift behavior of those lines.

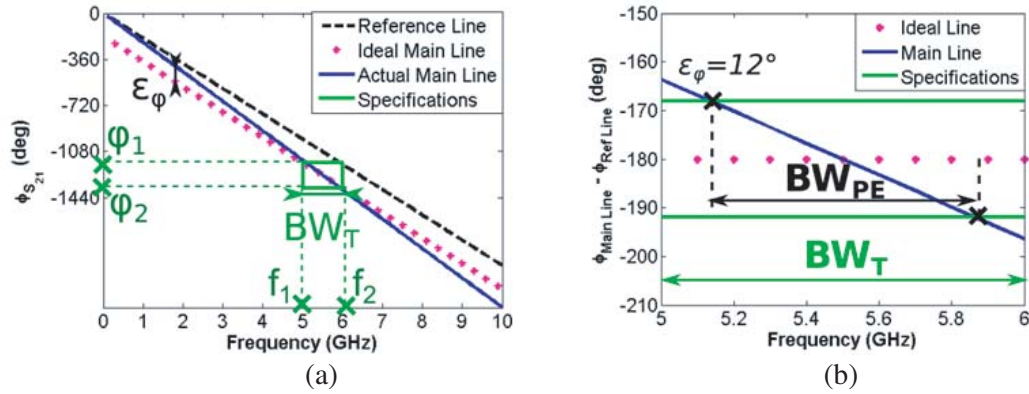


**Figure 2.** (a) Illustration of the difference in phase between an ideal main line of a DPS and its actual main line for a  $180^\circ$  TL DPS through their unwrapped phase behavior and (b) illustration of the phase error bandwidth  $BW_{PE}$  and targeted bandwidth  $BW_T$  for the same DPS with a tolerated phase error of  $\pm 12^\circ$ .

shift with respect to the reference line. The frequency bandwidth requested to get this phase shift will be called the targeted bandwidth  $BW_T$ . The phase shift criteria for metamaterial DPS are presently defined in this paper as two phase values (called in this article  $\varphi_1$  and  $\varphi_2$ ) referred as the targeted bandwidth  $BW_T$  boundaries ( $f_1$  and  $f_2$ ) as shown in Figure 2(a).

As seen in a basic instance of a TL DPS in Figure 2(a), the actual main line is compared to a theoretical ideal main line resulting from a shift of the reference line by the targeted phase shift over all frequencies. This shows that the main and reference lines have an unwanted phase shift at most frequencies and can only have the requested phase shift over a rather reduced frequency bandwidth. This issue is highlighted in Figures 2(a) and 2(b) where the actual and ideal main line have an almost equal phase shift for a quite reduced bandwidth.

The unwanted phase shift resulting from this behavior is called phase error  $\varepsilon_\phi$  and will be used as a criterion for the phase shift accuracy. Since this condition must be ensured over a specified bandwidth, the phase shift performance criterion will be defined as the bandwidth where the phase error  $\varepsilon_\phi$  is below a threshold of  $12^\circ$ , also called the phase error bandwidth  $BW_{PE}$  as illustrated in Figure 2(b). Unlike the  $BW_T$  which is considered as an input, the  $BW_{PE}$  corresponds to a variable output which needs to be adjusted. The aim of a DPS design is then to have a  $BW_{PE}$  which contains the  $BW_T$ . In order to integrate DPS for industrial applications, it needs to comply with a sufficiently low return loss ( $S_{11} < -15$  dB), which will be evaluated through the return loss bandwidth  $BW_{RL}$ . In the end, the full achieved bandwidth of the DPS will then be defined as the overall bandwidth  $BW_O$ , which is the intersection of the  $BW_{PE}$  and the  $BW_{RL}$ .

When conventional DPS based on transmission lines are used, the  $BW_{PE}$  value is quite limited, since the phase shift can only be corrected by changing the length of the main line according to a selected substrate. When a metamaterial replaces the standard transmission line, the additional number of degrees of freedom potentially enables an improved control of the phase, which results in a better control on the  $BW_{PE}$ . However, due to the high number of parameters of a metamaterial DPS, a dedicated design method is needed to get the right phase behavior.

## 2.2. Principle of the Design Method

In this paper, the design method, whose purpose is to minimize the full wave computation, is split in three steps as shown in Figure 3.

We start by developing a design method of a theoretical CRLH-TL from phase specifications by using equivalent circuit models. From then on, the second step is the conversion of this initial equivalent circuit into a 3D geometry that can be simulated by full wave EM software. The third and final step consists in the optimization of this initial 3D geometry to get the targeted phase.

One of the purposes of the method is to reduce calculation time to a minimum by decreasing as

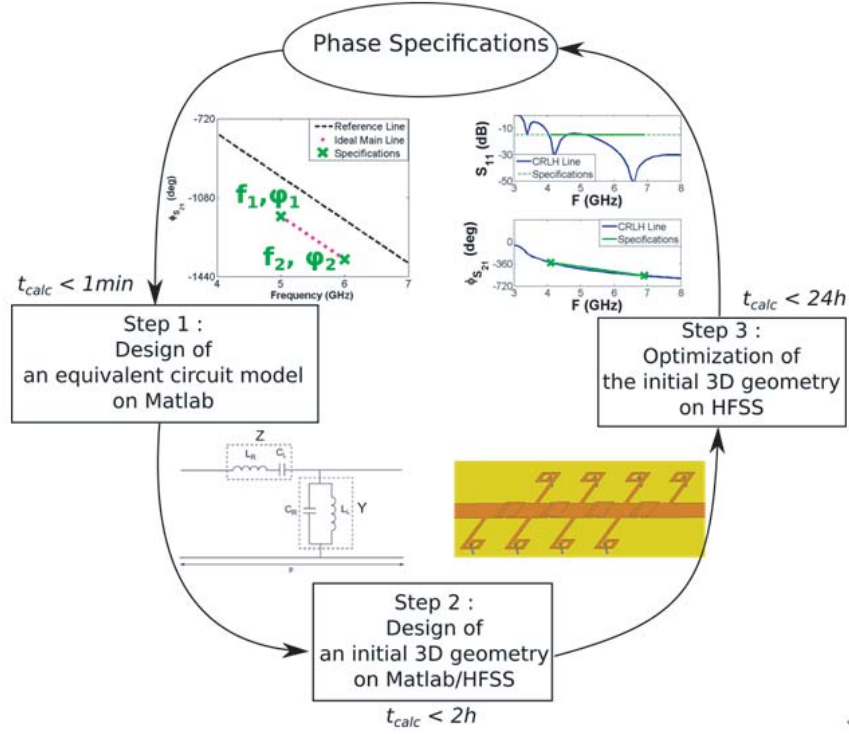


**Figure 3.** Flowchart of the general design method.

much as possible the number of runs of the 3D geometry optimization, which is a very time consuming process. The only way to achieve this goal is to design an initial 3D geometry as close as possible to the optimized design. This method also aids at designing metamaterial phase shifters with improved specifications for industrial applications. To this end, a new way of exploiting metamaterial parameters is used by considering central bandgap of unbalanced solutions as degree of freedom, to achieve better performances in terms of compactness and return loss. The theoretical formulas which led us to build this design method are then detailed in the following parts of this section.

### 2.3. Equivalent Circuit Model of the CRLH-TL

The CRLH-TL can be seen as a periodic structure composed of lumped and distributed electrical elements [5], and can be described by its lossless equivalent circuit elements such as in Figure 4. It can be considered as a transmission line, represented by its distributed elements, also called Right Handed, periodically loaded by lumped elements, also called Left Handed. The line can thus be simplified as a series of  $M$  identical unit cells, each composed of LH and RH elements, and its length, which will be used as compactness parameter, is  $l_{line} = M * p_{cell}$  with  $p_{cell}$  the unit cell length.

By expressing the  $ABCD$  matrix of this cell with electrical elements [5] to determine the  $S$  matrix of the line, the reflection gain ( $S_{11}, S_{22}$ ), transmission gain ( $S_{12}, S_{21}$ ), and the phase of the line ( $\varphi_{S_{21}}$ ) are obtained as displayed in Figure 5.

In Figure 5, the CRLH line reflection and transmission levels highlight how the line is working: a first propagation band, called the LH propagation band, is located between  $f_{c1}$  and  $f_{c2}$ , followed by a band gap between  $f_{c2}$  and  $f_{c3}$ , and another propagation band called the RH band between  $f_{c3}$  and  $f_{c4}$ . These cut off frequencies which can be determined through the lumped and distributed electrical elements [5] are used for generic design of CRLH lines.

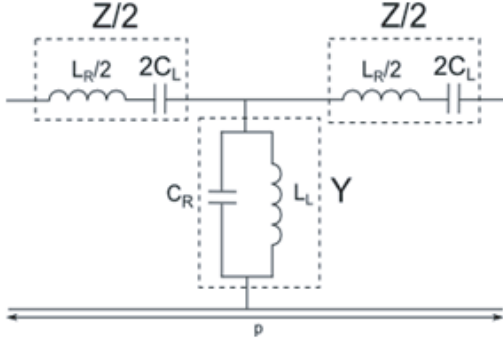


**Figure 4.** Equivalent circuit model for the CRLH TL unit cell.

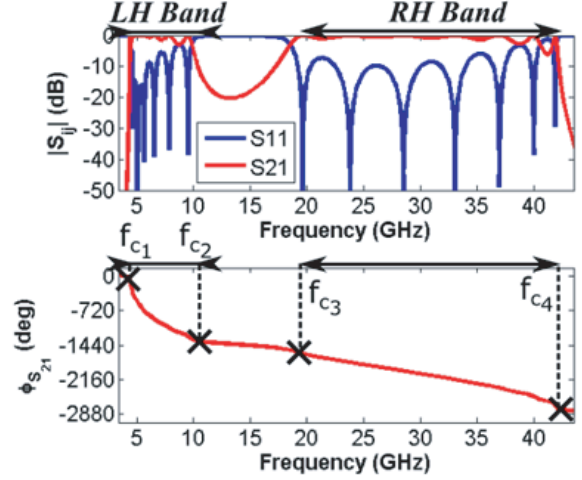


**Figure 5.** Magnitude of  $S_{ij}$  and phase of  $S_{21}$  for the equivalent circuit model of an 8 cells CRLH line.

#### 2.4. Electrical Element Derivation from Phase Specifications

In order to design a metamaterial line from two phase values, a link between the phase and electrical elements of the line needs to be established. It is not possible with the transmission phase since it is the result of a non-bijective matrix calculation. Consequently this calls for another phase definition.

For this purpose, a Bloch-Floquet [13] description of the line can be used to extract its theoretical phase by considering the line as an infinite periodic structure. This phase description has been developed and justified in a previous article [14] and can be summed up in a relation between two theoretical phase values ( $\varphi_1$  and  $\varphi_2$ ) and their respective frequencies values ( $f_1$  and  $f_2$ ) with the electrical elements of the line ( $C_L$ ,  $L_L$ ,  $L_R$ ,  $C_R$ ) for the particular case of a balanced CRLH-TL:

$$C_L = \frac{f_1^2 - f_2^2}{4\pi f_1 f_2 Z_R \left( f_1 \cos\left(\frac{\varphi_2}{2M}\right) - f_2 \cos\left(\frac{\varphi_1}{2M}\right) \right)} \quad (1)$$

$$L_L = Z_R^2 C_L \quad (2)$$

$$L_R = \frac{1}{4\pi^2 f_1^2 C_L} - \frac{Z_R}{\pi f_1} \cos\left(\frac{\varphi_1}{2M}\right) \quad (3)$$

$$C_R = L_R / Z_R^2 \quad (4)$$

Another parameter appears in these formulas: the RH impedance  $Z_R$  which can be seen as the characteristic impedance of the TL constructed only from the distributed elements. This impedance is fixed and corresponds to the reference impedance  $Z_0$  (in our case  $50 \Omega$ ).

#### 2.5. Definition of a Set of Unbalanced Lines Satisfying Phase Specifications

In Subsection 2.4, the existence of a CRLH-TL solution for a DPS design has been demonstrated. This was made possible by using the particular case of balanced lines and by adding the balanced condition to the actual system of equations. This being said, other solutions of this equations system built from phase specifications exist. They correspond to unbalanced lines with different central bandgaps.

Given that the aim of the design method is to get a phase shift over a targeted bandwidth  $BW_T$ , this bandwidth cannot contain any band gap. Hence the aimed phase shift has to be set in a unique propagation band (either LH or RH). However, to design from lumped elements the 3D components chosen in Section 3 for their low cost and ease of manufacturing, the lumped capacitance and inductance have to be of lowest values, which is the case with the LH band. Moreover, by definition of the CRLH-TL, an infinite number of unbalanced CRLH-TLs can exist with the same LH band, but with different

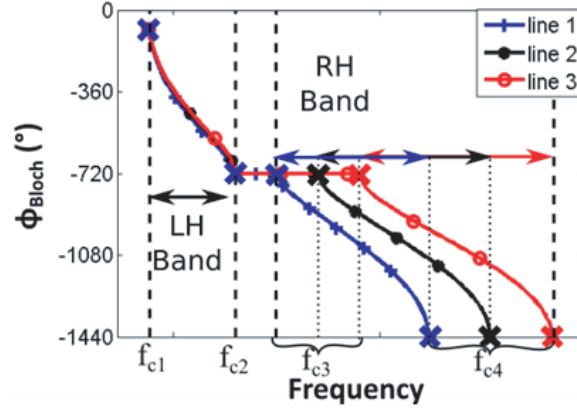


**Figure 6.** Comparison of the theoretical phase of three equi-LHCRLH-TLs.

central bandgaps and different RH band. Consequently, both LH band cut-off frequencies  $f_{c1}$  and  $f_{c2}$  can remain fixed while RH band cut-off frequencies  $f_{c3}$  and  $f_{c4}$  are changed.

Therefrom, we define a solution set, called equi-LH CRLH-TL, meeting the DPS phase specifications. This name refers to the fact that these solutions have the same LH propagation band but different bandgap and RH bands. This principle is illustrated in Figure 6, through a comparison of the phase behavior of three equi-LH CRLH-TLs. As previously noted, it is noticeable that the phase behavior of these 3 lines is the same inside the LH band and differs greatly in the RH band.

This innovative approach to design CRLH-TLs is implemented in our design method. This method enables the generating of multiple TLs using the same phase shift constraint in LH band. These different lines will have various band gaps, which will result in different couples of electrical elements and in different performance indicators, notably  $S_{11}$  and compactness.

### 3. DESIGN METHOD OF CRLH-TL FROM PHASE SPECIFICATIONS

In Section 2, the design method has been introduced, and its theoretical background has been explained to grasp the method outlines. Section 3 will give a complete understanding of the general design process by detailing the three steps of the method shown in Figure 3:

- Step 1 — Design of an initial circuit model — explained in Section 3.1
- Step 2 — Design of an initial 3D geometry — developed in Section 3.2

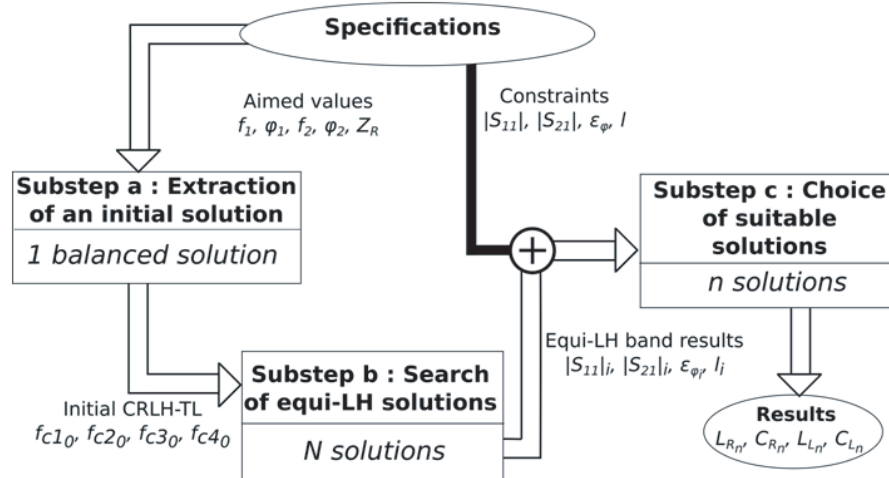


**Figure 7.** Flowchart of step 1 presented in Table 1.

- Step 3 — Optimization of the initial 3D geometry — expounded in Section 3.3

### 3.1. Step 1: Design of an Equivalent Circuit Model from Phase Specifications

The aim of this first step is to obtain a circuit model of CRLH-TL from phase specifications by using the formulas and circuit models previously developed in Section 2. The process of this first step is illustrated in the flowchart on Figure 7.

A unique initial balanced CRLH-TL is designed from the phase shift criteria as a result of the formulas seen in Section 2.4. Thereupon, from this first circuit model, a set of  $N$  equi-LH CRLH-TLs are extracted as explained in Section 2.5. Performances of these lines are then compared to the specifications, to only keep the  $n$  suitable cases.

The simulation time of step 1 takes less than one minute on a Matlab routine because it is based on equivalent circuit models. Indeed this step gives  $n$  equi-LH CRLH-TLs without using any full wave EM methods (i.e., FEM, FDTD or MoM).

### 3.2. Step 2: Equivalent Circuit Conversion into 3D Geometry

#### 3.2.1. Considered Approach

Step 2 consists in converting the equivalent circuit model in a 3D geometry which can be simulated in HFSS environment.

The circuit model that was designed in Section 2 is composed of distributed and lumped electrical elements. The distributed elements ( $L_R, C_R$ ) are converted into a uniform transmission line described in 3.2.2. On the other hand the lumped elements ( $L_L, C_L$ ) can be converted in 3D inductor and capacitor through structures that are described in 3.2.3. This conversion is done by transforming the electrical parameters of the circuit model into different kinds of geometrical parameters, such as: Metal-Insulator-Metal (MIM) capacitor length, stub inductor length and length and width of the uniform TL.

These representations of electrical elements are shown in a simplified schematic design of the 3D geometry in Figure 8. In order to keep the symmetry of the line, the electrical elements are split in a symmetric II or T-network. As this design is purely schematic, the choice of T or II design can be interchanged if necessary, particularly if the lumped elements are unmanufacturable due to the current fabrication norms.

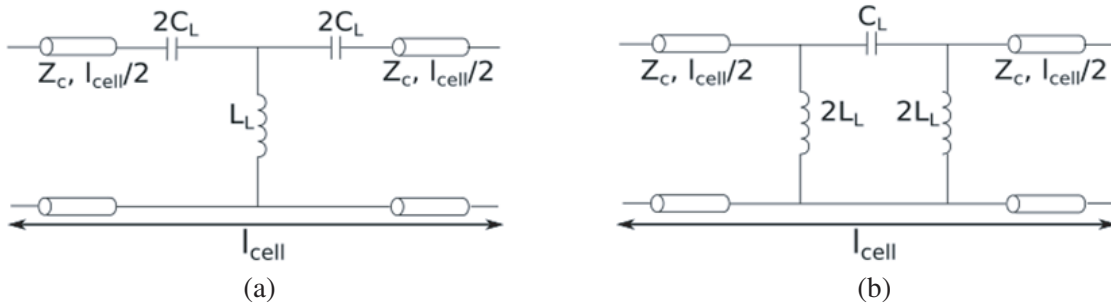


**Figure 8.** Equivalent circuits of a CRLH-TL unit cell: in (a) T-network and (b) II-network.

#### 3.2.2. Distributed Elements Design

The distributed elements are directly related to the characteristic impedance  $Z_c$  of the transmission line:

$$Z_c = \sqrt{\frac{L_R}{C_R}} \quad (5)$$

To convert this impedance in geometrical parameters, the type of transmission line needs to be specified. In this paper, the transmission line chosen to embody distributed elements is the microstrip

line by virtue of its ease on a designing and a manufacturing levels. The length  $L_{\text{line}}$  and width  $W_{\text{line}}$  of the line can then be obtained from the defined characteristic impedance  $Z_c$  and substrate height  $h$  and permittivity  $\varepsilon_r$  [15].

### 3.2.3. Lumped Elements Design

Each lumped element can be associated to an equivalent 3D capacitance or inductance [16], and its electrical parameters can be converted in geometrical parameters. The choice of technological implementations used is highly relying on the frequency range considered (in this paper, C-Band) and the TL technology (microstrip).

The MIM capacitor (Figure 9) has been chosen in this article as a lumped capacitor for its simplified equivalent circuit model with a broad validity range.

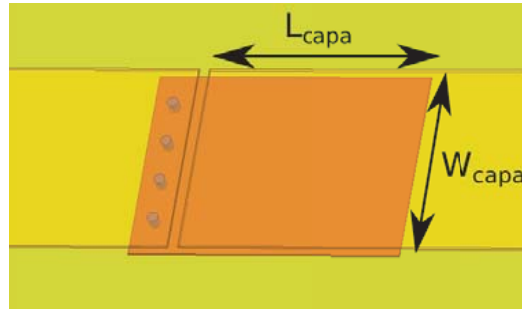


**Figure 9.** View of MIM capacitor.

To choose the inductance, simple implementations such as short-circuit shunt stub inductor (Figure 10(a)) have been investigated as well as more complex implementations with spirals (Figure 10(b)). The shunt stub is the easiest one to design, yet with the lowest values of inductance. The spiral geometry can achieve higher values by extending the electric length but its equivalent circuit is less established.

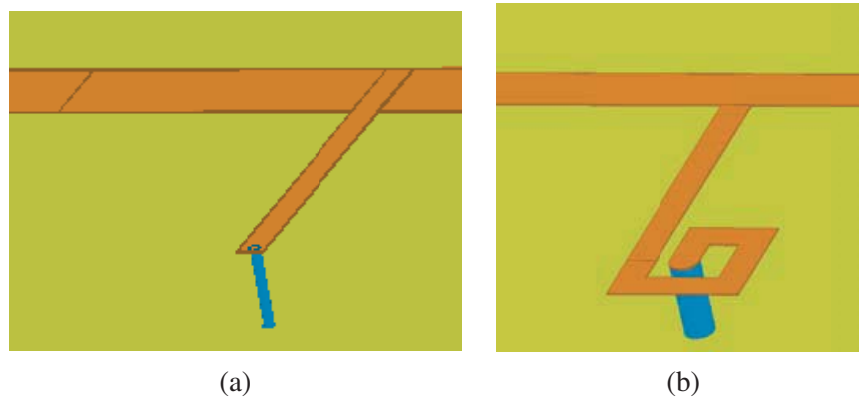


**Figure 10.** (a) Views of short-circuit shunt stub inductor, (b) short-circuit shunt stub inductor with spiral.

### 3.3. Step 2: 3D Geometry Design

The geometrical model design purpose is to convert LH and RH electrical elements in a geometrical structure of equivalent performances coupled with a time-efficient process. This conversion is done,

theoretically, by using the equivalent circuit models of the desired 3D elements. However some discrepancies can be observed for some elements, especially LH elements corresponding to the most inaccurate models.

This is why, in our method, a simplified equivalent circuit is established for a first set of geometrical parameters needed for the initial HFSS simulation. This is then followed by a reverse calculation step between the  $S$ -parameters of the single LH element simulated on HFSS and  $S$ -parameters of the equivalent circuit model. It is notable that the full-wave simulations are only done on one 3D element at a time.

This method, illustrated in Figure 11, ensures a very resembling 3D geometry, with the same behavior as the equivalent circuit and a time efficient process.

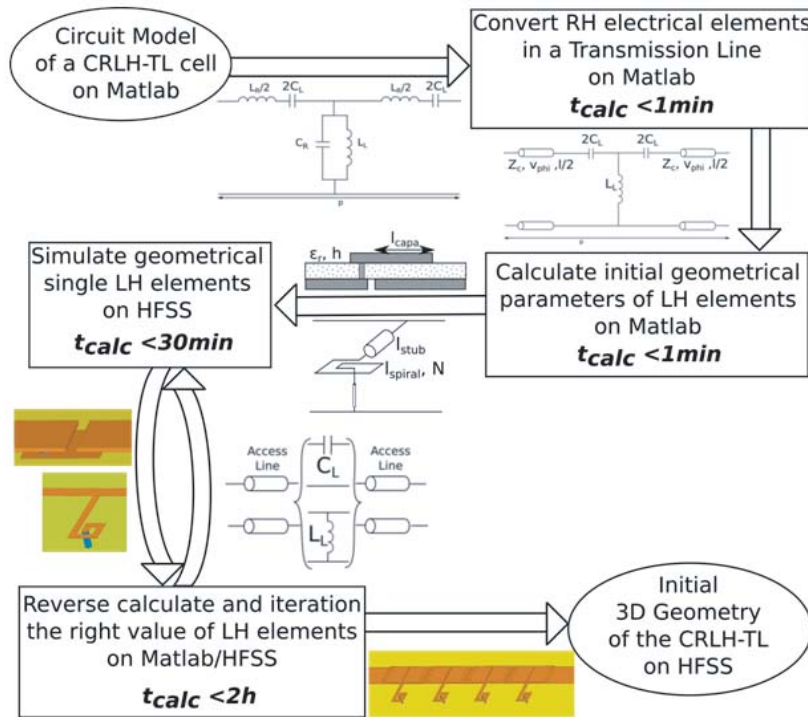


**Figure 11.** Flowchart of the design method of the 3D geometry of the CRLH-TL from its equivalent circuit model.

With more time and resources, this last step of reverse calculation can be replaced by a step of reverse engineering, for which each LH element is fabricated and measured with an adequate number of samples to secure accurate performances.

### 3.4. Step 3: Optimization Process

The last step of the design method in Figure 3 is the optimization process on HFSS of the line designed and simulated in Subsection 3.3. This is a necessary step to correct the phase error and the return loss error accumulated through equivalent circuit model simplifications, parasitic resonances, and coupling neglected in theoretical models.

This optimization process will be carried out by varying for each 3D element (LH capacitance, LH self, and RH host line), its most influencing parameter making this process a three-variable parametric study. Knowing that the initial 3D geometry parameters are not far from parameters which will give a solution with adequate performances, the parametric study shall be carried out at the vicinity of the initial case by varying each of the chosen geometrical parameters independently. Consequently for each of the three parameters, two steps will be executed by making each parameter varying of  $\pm\alpha\%$ .

In this fashion, this study gives a result of seven simulated designs: the initial design and six deviations of one parameter of  $\pm\alpha\%$ . In cases where none of the designs have adequate performances, an interpolation of the phase error and return loss results among the defined variables makes possible to find a solution in another set of designs (six other simulations). This process is made possible by the two first steps of the design method which led to an initial solution close to the aimed result, as demonstrated later in Section 4.5.

#### 4. APPLICATION: 20% BANDWIDTH CRLH-TL 180° PHASE SHIFTERS IN C-BAND

##### 4.1. Analysis of Delay Lines Limits

To illustrate the design method developed in Sections 2 and 3, we designed a direct application of CRLH-TL DPS at C-band (5–6 GHz). The purpose of this application was to design a DPS with a 20% targeted bandwidth  $BW_T$  ( $S_{11} < -15$  dB and  $\varepsilon_\varphi < 12^\circ$ ), and with an insertion loss suited for industrial application ( $S_{21} < 1$  dB). To this end, the performances of the line are evaluated on this  $BW_T$  of 20% and their actual  $BW_{PE}$  is calculated on this bandwidth, the ideal being a  $BW_{PE}$  wider than the  $BW_T$ . Moreover the overall bandwidth  $BW_O$  will also be calculated by taking into account  $S_{11}$  behavior to evaluate the actual performances of the DPS.

Phase specifications were chosen to be the hardest to satisfy for a standard TL DPS: we decided to design a 180° DPS composed of two TLs of different lengths on a same substrate. Indeed, due to their different lengths, the two lines have a different phase slope, resulting in a narrower phase error bandwidth  $BW_{PE}$  as the specified phase shift between these lines increases until reaching its highest value of 180° [360°].

In our case, the simulated simple microstrip line solution achieves a maximum phase error over the 20% bandwidth of  $\pm 20^\circ$  (Figure 12), and its  $BW_{PE}$ , centered around 5.5 GHz is of only 14% for a targeted  $\varepsilon_\varphi$  of  $\pm 12^\circ$ . Since it is a microstrip line, its insertion loss is under specifications for considered frequencies, and its  $BW_O$  equates to its  $BW_{PE}$ .

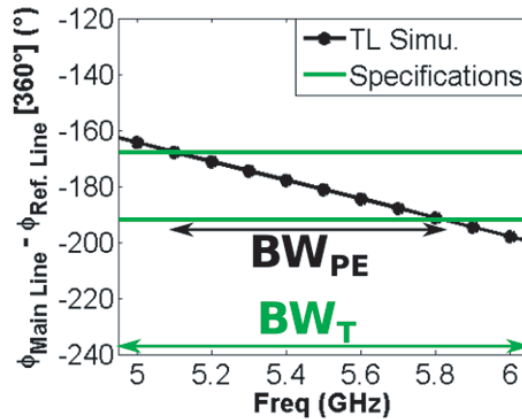


**Figure 12.** Differential phase shift performances of a 180° TL DPS for a BWT of [5–6 GHz].

##### 4.2. Design and Simulation of the CRLH-TL Phase Shifters

Designing the CRLH-TL phase shifter was done following the method we developed above.

For illustration, 3 cases of equi-LH-CRLH-TLs have been designed: a balanced case (0LH-CRLH-TL), a case with a 2 GHz bandgap (2LH-CRLH-TL) and a case with a 4 GHz bandgap (4LH-CRLH-TL). The last one is the most compact line, but is the hardest to design since the RH elements are of lowest value, which means that the unit cell is of smallest length, and the LH elements are of highest value, which means that the lumped structures have the biggest size, making the insertion into the unit cell rather difficult.

The choice of  $\Pi$  or T-Network was made depending on the capacitance: a T-Network was used for the 0LH-CRLH-TL and 2LH-CRLH-TL, but the double MIM capacitor could not be contained in the 4LH-CRLH-TL unit cell, so a  $\Pi$ -network was used instead. Stub inductors provide adequate inductance value for the T-Network needs, but for  $\Pi$ -Networks, the inductance value needs to be doubled. In this regard, spiral inductors are chosen. The lines were designed (Figure 13) and fabricated using a Rogers RT/duroid 5880 substrate with a relative permittivity of  $\epsilon_r = 2.2$  and a thickness of  $h = 508 \mu\text{m}$ .

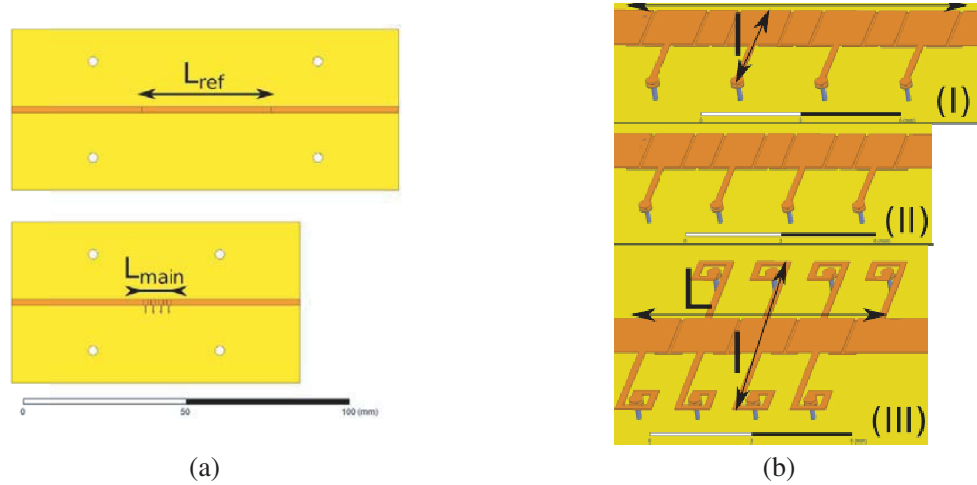


**Figure 13.** (a) Top view of the reference line (above) and one of the CRLH-TL main line at the same scale, (b) zoomed 3D-view of 0LH-T-Stub (I), 2LH-T-Stub (II) and 4LH-Spiral (III) designs on HFSS.

To add the MIM capacitors, a prepreg FR4 with  $\epsilon_r = 3.9$  and  $h = 50 \mu\text{m}$  was used as upper substrate (MIM dielectric) and attached to the main substrate with the help of a prepreg fast rise FR-27 with  $\epsilon_r = 2.42$  and  $h = 25 \mu\text{m}$ . This topology was included in HFSS designs to ensure the best prediction of real circuit behavior. The reference line was chosen with a length  $L_{ref}$  of 40 mm, as shown in Figure 13 in a top view of a DPS design, the main line and the reference line being surrounded by access lines to avoid any interactions with connectors. The simulated CRLH-TL line length  $L_{main}$  is between 7 and 12 mm depending on the central bandgap of the line, whereas for the simple microstrip simulated solution, the line length  $L_{main}$  is of 60 mm.

Once the lines are simulated and optimized conforming to our design method, a panel of results can be extracted as shown in Table 1. As opposed to the standard TL, the CRLH-TLs maintain a minimal phase error over the 20% bandwidth while keeping satisfying return and insertion losses. Our results also reveal that the CRLH-TLs are, as expected, a lot more compact compared to the TL DPS. The lines with higher bandgap have similar return loss and phase shift performances than the balanced case (0LH) while having a smaller length but larger width which is only caused by the change of network. These results show that multiple equi-LH TLs can be built for a specific phase shift requirement, with different performances, with or without emphasizing compactness.

**Table 1.** Performances of each simulated line over the fixed 20% bandwidth of 5–6 GHz (out of specs performances in grey).

Geometry	Max( $S_{11}$ ) (dB)	Min( $S_{21}$ ) (dB)	Max( $\epsilon_\phi$ ) ( $^\circ$ )	Area ( $L^*l$ ) (mm*mm)
0LH-T-Stub	-20	-0,3	5,5	11*4
2LH-T-Stub	-20	-0,3	6,2	10*4
4LHPI-Spiral	-21	-0,3	5,3	7*8
Standard TL	-36	-0,1	19,6	60*2

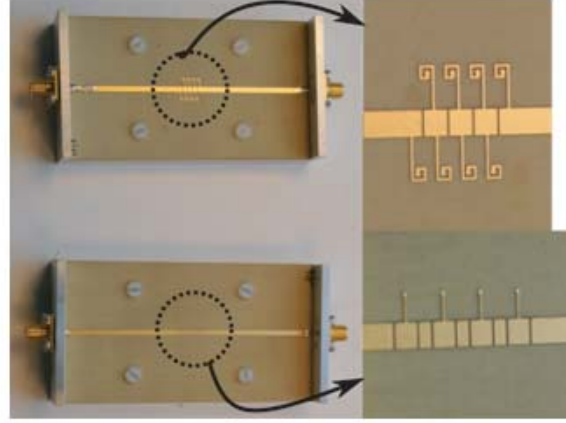


**Figure 14.** Photograph of the fabricated prototypes, 4LH-II-Spiral at the top and 2LH-T-Stub at the bottom.

### 4.3. Experimental Results of the CRLH-TL Phase Shifters

Figure 14 shows a picture of some of the prototypes. The lines were fabricated along with a TRL calibration kit for phase shift measurement precision, composed of two straight microstrip lines with a differential phase shift of  $90^\circ$  (T and L) and a double shorted line, called the Reflect Line (R). These prototypes were characterized with a Vector Network Analyzer ZVA67 Rohde&Schwarz, and their performances are exposed in Table 2.

**Table 2.** Performances of each realized line between 5 and 6 GHz (out of specs performances in grey).

Geometry	Max( $S_{11}$ ) (dB)	Min( $S_{21}$ ) (dB)	Max( $\epsilon_\phi$ ) ( $^\circ$ )	Area ( $L^*l$ ) (mm*mm)
0LHT-Stub	-16	-1.1	11.3	11*4
2LHT-Stub	-14	-1.0	8.6	10*4
4LH-PI-Spial	-16	-0,9	24.3	7*8
Standard TL	-25	-0,4	30.2	60*2

The 0-LH-T-Stub TL meets all the specifications except insertion losses a little less ( $-1, 1$  dB) than expected. The 2-LH case has the lowest phase error ( $8.6^\circ$ ) but a return loss slightly above the required value ( $-14$  dB). Even if these two lines reach the limit of specifications for return loss or insertion loss, they show very good performances on the considered bandwidth overall. As for the 4LH-PI Spiral TL and the standard TL, they do not comply with the phase specifications. These results will be further explained and compared with the simulation results in the next section.

### 4.4. Discussion of the Results

Firstly, it is notable in Figure 15 that the standard DPS based on microstrip line alone has a significant phase error offset compared to the simulations ( $30.2^\circ$  for the realized line compared to  $19.6^\circ$  for the simulated one). This may be caused by a modeling approximation, due to design simplification of the substrates' stacking and bonding on HFSS. This minor deviation is amplified by the line length of 60 mm. Due to their shorter length line, the effect can be neglected in the metamaterials' case.

In Figure 15, CRLH-TL performances with stub inductor reveal that the measured and simulated results match and are both compliant with the specification. In particular, the 2-LH CRLH-TL has a maximum phase error of  $8.6^\circ$  across the defined 20% bandwidth, a very low phase shift variation along the bandwidth, and a return loss only slightly below specification at the right edge of the bandwidth.

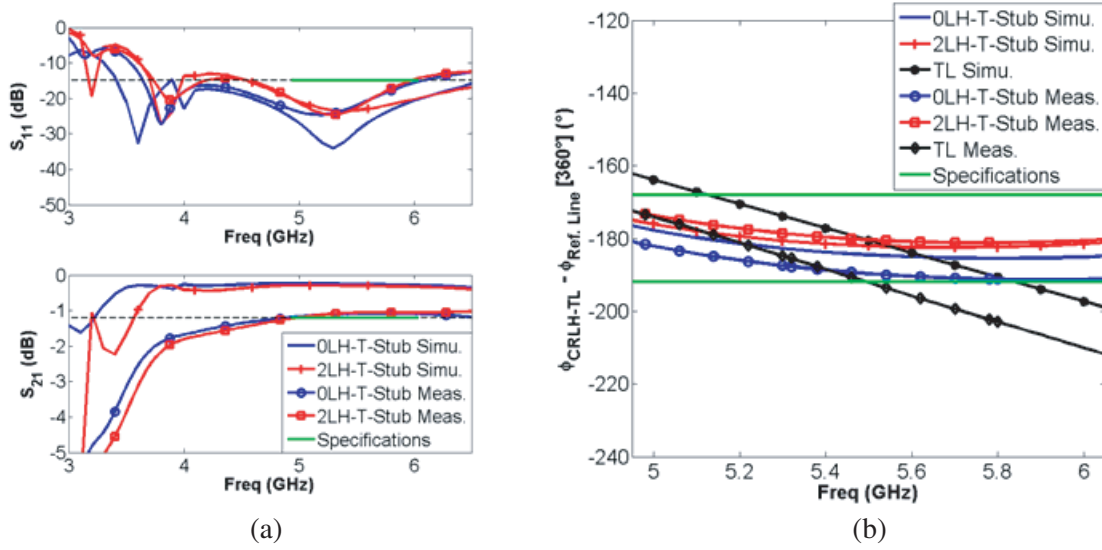


**Figure 15.** 0LH, 2LH-T-Stub CRLH-TLs and simple TL performances in terms of (a)  $S_{11}$ ,  $S_{21}$  and (b) differential phase shift within the  $BW_T$ .

In the case of the 4LH-CRLH-TL with spiral inductors, the prototype keeps showing good return and insertion loss (Figure 16(a)), but we can observe a phase shift between simulated and measured results (Figure 16(b)). This is caused by the complexity of the spiral inductor geometry used for this line, and can be solved using the reverse engineering process discussed in III-D, which will lead to a more accurate equivalent circuit model.

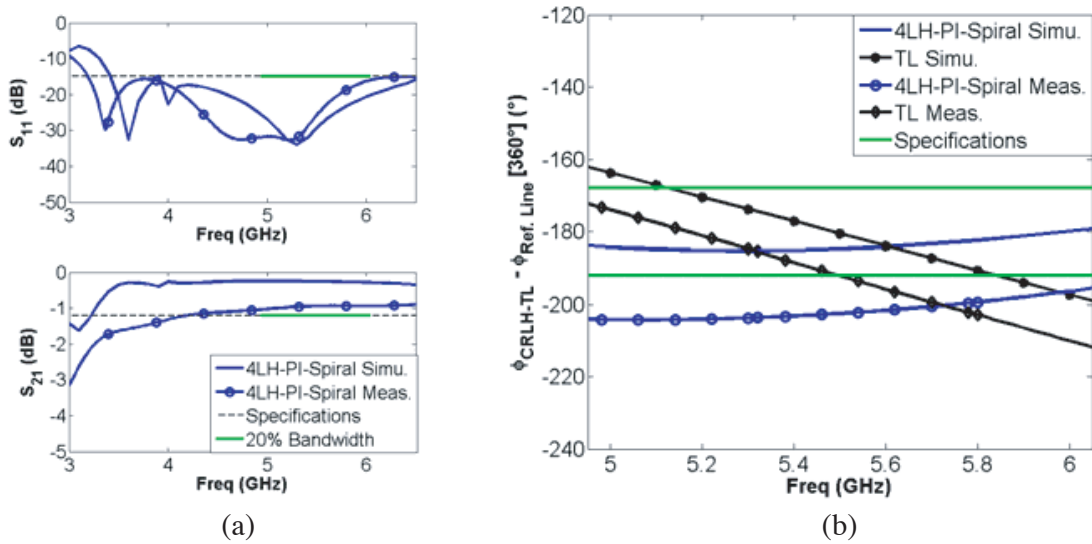


**Figure 16.** 4LH-PI-Spiral CRLH-TL and simple TL performances in terms of (a)  $S_{11}$ ,  $S_{21}$  and (b) differential phase shift within the  $BW_T$ .

Since the 0LH and 2LH-T-Stub cases present a phase shift response above specifications along the entire  $BW_T$ , we performed a study of their actual  $BW_{PE}$  and  $BW_O$ .

The results presented in Figure 17 reveal that the realized prototype (here 2LH-T-Stub) achieve good phase performances beyond the expected  $BW_T$ . As shown in Table 3, its  $BW_{PE}$  is of 38% for the 2LH-T-Stub and 49% for the 0LH case, as opposed to the TL case which is of only 15%.

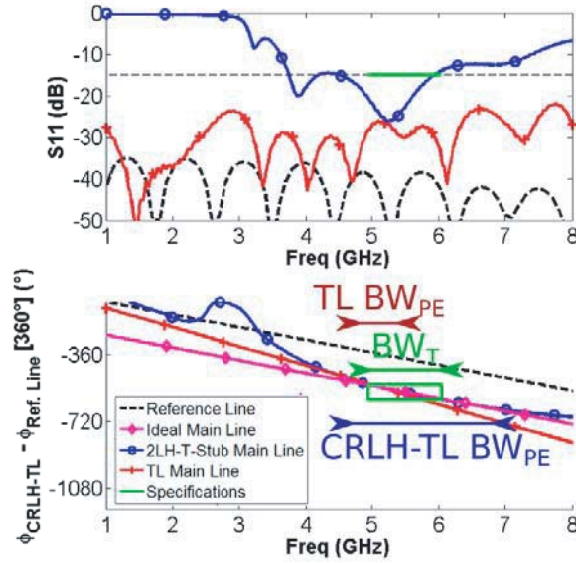


**Figure 17.** 2LH-T-Stub CRLH-TL and simple TL performances in terms of  $S_{11}$  and phase shift.

**Table 3.** Performances of each realized line regarding to their different achieved bandwidth ( $BW_{PE}$ ,  $BW_{RL}$ ) and total bandwidth ( $BW_O$ ).

Geometry	$BW_{PE}$ (GHz)	$BW_{PE}$ (%)	$BW_{RL}$ (GHz)	$BW_{RL}$ (%)	$BW_O$ (GHz)	$BW_O$ (%)
0LHT-Stub	4.5-7.4	49	3.7-6.0	48	4.5-6.0	29
2LHT-Stub	4.7-6.8	38	4.5-5.9	27	4.7-5.9	23
4LHPI-Spi	6.2-7	13	3.8-6	44	-	0
Standard TL	4.8-5.5	15	0.1-10	-	4.8-5.5	15

Since the return loss is higher than  $-12.5$  dB in this band for the 2LH-T-Stub and higher than  $-10$  dB for the 0LH case, their actual  $BW_O$  is narrower, but those lines still exhibit better performances than the TL case. It supports the possibility of using the CRLH TL non-linear phase behavior for wideband DPS applications, applying the currently described design method.

These results also demonstrate that it is possible to achieve a phase shift control on larger bandwidth than the targeted 20% of our application.

In order to further improve phase shift performances, it would be possible to make the reference line a CRLH-TL too, using the same method than we did with the main line. We would then get a higher number of parameters, making it possible to obtain the same non-linear phase behavior for both lines, ensuring a wideband phase shift control.

#### 4.5. Examination of the Method Time-Efficiency

In order to assess the time saved using our design method, we proceeded as follows: we compared the number of HFSS simulations we ran to get a satisfying result with a parametric study, initialized with a 3D geometry generated by a regular method.

As a means to avoid unmanageable and time-consuming simulations, we worked under certain assumptions: we kept the same substrate, cell length and cell number than those used for our experiment, and we chose the same implementation for the LH elements.

The remaining variables are the inductance and capacitance geometrical parameters, which can be assembled into two parameters: inductance and capacitance electric value. To do so, each structure was separately simulated to link its diverse geometrical parameters to a unique electrical parameter.

This leads to a parametric study of ten runs for each parameter to reach all the realistic possibilities for every corresponding structure, amounting to a 100 simulations. This rather optimistic target number has to be considered for a purpose of simplified comparison with our parametric study, meaning that in a real case, a larger number of parameters which are not considered here would be implemented in the study, such as the substrate properties, the number of cells and the line length, making the parametric study much heavier than the one presented here.

The results of these simulations are exposed in Figure 18. The optimization process operated with our design method is represented by a white square, and the parametric study is illustrated by dotted black squares filled accordingly to their performances. In the 0LH case, we can observe that the optimization process already gives a satisfying solution.

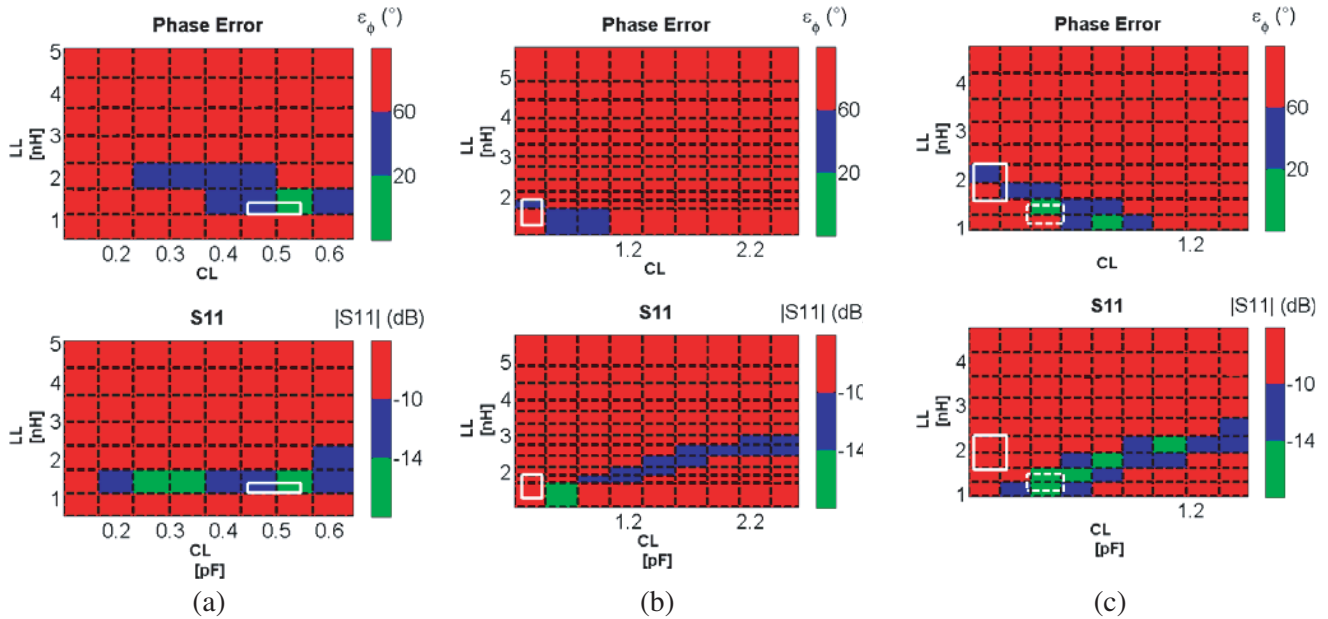


**Figure 18.** Optimization process graphs: comparison for (a) 0LH, (b) 2LH and (c) 4LH CRLH-TL geometries.

In the 2LH case, the design method optimization process is very close to the lines with the best performances, so that a simple extension of the process in the right direction can enable to obtain an optimized line.

As for the 4LH case, the optimization process is relatively far from the optimal results. However, the phase error variation among results makes possible to predict only one more process (dotted white square) to find an acceptable solution.

In conclusion, a solution with adequate performances can be obtained through our optimization process with only 7 to 15 full wave simulations, while 100 simulations are required for the given generic study. In a realistic case, no assumptions can be made at the beginning, resulting in a far more demanding process in terms of resources than this 100 simulations sample.

This study illustrates the time gained using our design method compared to a more general parametric study: the initial 3D geometry designed on HFSS is indeed very close to the area of suitable solutions. Moreover, the more we increase the bandgap of the metamaterial, the higher the number of iterations will be needed to find a good solution, even though predictions can still assure a time efficient process.

## 5. CONCLUSION

This section summarizes the findings and contributions made, based upon our innovative way of using metamaterial properties for the design of compact and wideband differential phase shifters. This method uses both balanced and unbalanced CRLH-TL through a concept called equi-LH lines, which consists in CRLH-TLs with an equivalent LH band but with different RH bands.

This concept has been implemented in a dedicated time efficient design method which converts phase specifications in a particular case of balanced CRLH-TL leading to a set of equi-LH lines. Each solution gives a different return loss and a different size corresponding to specific application.

This method was used in this paper to design three prototypes of CRLH-TL applied to a 20% bandwidth DPS in C-Band, taking into consideration industrial constraints for an application in RF payloads. Superior results were achieved with it, even better than those predicted in terms of  $BW_{PE}$  (49% for the 0LH case and 38% for the 2LH one with a return loss of more than  $-10$  dB) with suitable results for the  $BW_{RL}$  for two prototypes. The compactness and  $BW_O$  improvements are spotlighted not only by a comparison with a microstrip DPS but also by the comparison between different equi-LH lines.

The result now provides evidence to the interest of using unbalanced lines to get more compact designs with same phase performances. It has also demonstrated the time efficiency of our dedicated method, thanks to the design of an initial 3D geometry with parameters close to the optimized geometry ones.

## ACKNOWLEDGMENT

The authors acknowledge the infrastructure and support of ONERA, the French Aerospace Lab, Toulouse, France and Thales Alenia Space, Toulouse, France. The authors thank B. Gabard for his help on the fabrication of the prototypes and the measurements and V. Gobin for his help during the writing of this paper. The authors appreciate T. Girard and Y. Cailloce's valuable and profound comments on industrial applications. The authors would like to thank B. Kan for the language editing.

## REFERENCES

1. Schiffman, B. M., "A new class of broad-band microwave 90-degree phase shifters," *IRE Transactions on Microwave Theory and Techniques*, Vol. 6, No. 2, 232–237, Apr. 1958.
2. Ellinger, F., H. Jackel, and W. Bachtold, "Varactor-loaded transmission-line phase shifter at C-band using lumped elements," *IEEE Transactions on Microwave Theory and Techniques*, Vol. 51, No. 4, 1135–1140, Apr. 2003.
3. Lin, Y. W., Y. C. Chou, and C. Y. Chang, "A balanced digital phase shifter by a novel switching-mode topology," *IEEE Transactions on Microwave Theory and Techniques*, Vol. 61, No. 6, 2361–2370, Jun. 2013.
4. Veselago, V. G., "The electrodynamics of substances with simultaneously negative values of  $\epsilon$  and  $\mu$ ," *Soviet Physics Uspekhi*, Vol. 10, No. 4, 509–514, Jan.–Feb. 1968.
5. Caloz, C. and T. Itoh, "TL theory of MTMs," *Electromagnetic Metamaterials: Transmission Line Theory and Microwave Applications*, 59–132, Wiley, Nov. 2005.
6. Eleftheriades, G. V. and K. G. Balmain, "Negative-refractive-index transmission-line metamaterials," *Negative-Refractive Metamaterials — Fundamental Principles and Applications*, 1–48, Wiley, Aug. 2005.
7. Zvolensky, T., J. Ala-Laurinaho, C. R. Simovski, and A. V. Raisanen, "A systematic design method for CRLH periodic structures in the microwave to millimeter-wave range," *IEEE Transactions on Antennas and Propagation*, Vol. 62, No. 8, 4153–4161, Aug. 2014.
8. Chi, P.-L. and T. Itoh, "Miniaturized dual-band directional couplers using composite right/left-handed transmission structures and their applications in beam pattern diversity systems," *IEEE Transactions on Microwave Theory and Techniques*, Vol. 57, No. 5, 1207–1215, May 2009.

9. Antoniadou, M. A. and G. V. Eleftheriades, "Compact linear lead/lag metamaterial phase shifters for broadband applications," *IEEE Antennas and Wireless Propagation Letters*, Vol. 2, No. 1, 103–106, 2003.
10. Church, J., J. Meloling, and J. D. Rockway, "Equal phase slope metamaterial transmission lines," *2012 IEEE Antennas and Propagation Society International Symposium (APSURSI)*, 1–2, Nov. 2012.
11. Siso, G., M. Gil, J. Bonache, and F. Martin, "Application of metamaterial transmission lines to design of quadrature phase shifters," *Electronics Letters*, Vol. 43, No. 20, 1098–1100, Sep. 2007.
12. Qamar, Z., S. Y. Zheng, W. S. Chan, and D. Ho, "An equal-length multiway differential metamaterial phase shifter," *IEEE Transactions on Microwave Theory and Techniques*, Vol. 65, No. 1, 136–146, 2017.
13. Collin, R. E., "Periodic structures and filters," *Foundations for Microwave Engineering*, 550–559, Wiley, 2000.
14. Vivos, J., T. Crépin, M. F. Foulon, and J. Sokoloff, "Design method of CRLH TL inspired phase shifters," *2016 10th European Conference on Antennas and Propagation (EuCAP)*, 2016.
15. Bahl, I. and P. Bhartia, "Transmission line theory," *Microwave Solid State Circuit Design*, Ch. 2, 12–21, 45–57, Wiley, 1988.
16. Bahl, I., *Lumped Elements for RF and Microwave Circuits*, 17–161, 163–251, Artech House, Apr. 2002.